Hexanediamine Monolayer Electrografted at Glassy Carbon Electrodes Enhances Oxygen Reduction Reaction in Aqueous Neutral Media

View the article online for updates and enhancements.

Hexanediamine Monolayer Electrografted at Glassy Carbon Electrodes Enhances Oxygen Reduction Reaction in Aqueous Neutral Media

Hairul Hisham Hamzah,[1,z] **Najahtul Najihah Ahmad Kamal,[1]** **Marta Meneghello,[2]** **Saiful Arifin Shafiee,[3]** **Turgut Sönmez,[4,5]** **Mohamad Nurul Azmi Mohamad Taib,[1]** **Shazarizul Haziq Mohd Samsuri,[6]** and **Meor Faisal Meor Zulkifli[7]**

[1]*School of Chemical Sciences, Universiti Sains Malaysia, 11800, Gelugor, Penang, Malaysia*
[2]*Aix-Marseille Université, CNRS, BIP UMR 7281, 31 Chemin J. Aiguier, 13009 Marseille, France*
[3]*Department of Chemistry, Kulliyyah of Science, International Islamic University Malaysia, Jalan Sultan Ahmad Shah, 25200 Kuantan, Pahang, Malaysia*
[4]*Department of Energy Systems Engineering, Technology Faculty, Karabük University, 78050 Karabük, Turkey*
[5]*Institut für Technische und Makromolekulare Chemie, RWTH Aachen University, Worringerweg 2, 52074 Aachen, Germany*
[6]*TNB Research Sdn Bhd., 43000, Kajang, Selangor, Malaysia*
[7]*iNeurons, Tower 5, Sky Park, 47100, Cyberjaya, Selangor, Malaysia*

This study presents for the first time the electrocatalytic behaviour of hexanediamine (HDA) monolayer electrografted at glassy carbon (GC) electrodes that enhanced oxygen reduction reaction (ORR) in aqueous neutral media. HDA modified GC electrodes gave a higher current density than platinum bare electrodes based on the cyclic voltammograms (CV), although a $\sim$0.21 V *vs.* Ag/AgCl higher onset potential was observed at -0.1 mA cm^{-2}. Electrochemical impedance spectra (EIS) showed that the electrocatalytic reaction on HDA monolayer film towards dissolved oxygen molecules is controlled by diffusion and charge transfer processes. From the scan rate studies and the Laviron equation, it was found that the ORR on this modified electrode proceeded via a fast four-electrons transfer.

Electrografting consists of an electrochemical reaction that allows organic layers to bind to a solid conducting surface. This reaction generally results in the formation of covalent bonds between the electrode surface and the organic molecules.[1,2] Electrografting of primary amine linkers is a widely used technique for electrode modification to covalently immobilize redox molecules or biomolecules onto the electrode surface.[3–5] The electrochemical attachment of primary amines at carbon electrodes is an efficient method since a strong carbon-nitrogen bond is formed during the one-electron oxidation of the amine.[6,7] Electrografting has received increasing attention due to its potential application in the development of electrochemical devices, given that uniform and highly stable organic monolayers can be formed. In addition, electrografting brings new properties to the modified surface and allows the immobilization of different redox active molecules to the electrode.[8,9] However, to the best of our knowledge, there are still no studies reported on the potential of electrografted primary amines as an electrocatalyst for oxygen reduction reaction (ORR).

Recently, Bartlett et al. have shown that a stable attachment of engineered enzymes to maleimide-modified multi-walled carbon nanotube (MWCNT) electrodes can be achieved through the electrografting of a primary amine, such as hexanediamine (HDA).[5,10,11] In their work, HDA acts as a linker to further functionalize the MWCNT electrodes. Monolayers of HDA linkers were immobilized on MWCNT electrodes through the electrochemical oxidation of mono-Boc-protected HDA in acetonitrile, where Boc (*tert*-butyloxycarbonyl) is a protecting group that allows the formation of a HDA monolayer at the electrode surface, preventing the grafting of the diamine linker to the GC surface on both ends, hence allowing for further functionalization after deprotection. After the deprotection of the electrografted HDA linkers by removal of the Boc group in an acid solution, solid-phase synthesis can be employed to affix a wide range of redox and enzyme molecules to the amino-modified electrode surface. One interesting study from Bartlett and co-workers is the immobilization of an enzyme at maleimide-modified electrodes (bilirubin oxidase, BOD) which results in the electrocatalytic reduction of O_2 through direct (unmediated) electron transfer from the electrode.[11]

In our work, after the Boc removal, we found that HDA films grafted at GC electrodes remarkably exhibit electrocatalytic activities toward the ORR in 0.1 M potassium chloride (KCl) and phosphate buffer (pH 7) solutions, even in the absence of immobilized enzymes or redox mediators. This makes the findings reported herein to be significantly novel in terms of ORR studied in aerated O_2 solutions using electrografted primary amines. Since we perform CV measurements in stagnant conditions, the number of transferred electrons (n) and kinetics involved in the ORR at the HDA monolayer grafted at GC electrode were determined using the Laviron equation for irreversible CV behaviours, which is a well-established method to calculate the electrode kinetics of redox molecules in stagnant conditions.

Experimental

Materials.—All reagents were used as received without further purification. Acetonitrile (CH$_3$CN, 99.9%), 1,4-dioxane (99%), hydrochloric acid (HCl, 37%) and potassium chloride (KCl, >99%) were acquired from Fisher Scientific. *N*-Boc-1,6-hexanediamine (>98%) was bought from Sigma Aldrich. Tetrabutylammonium tetrafluoroborate (TBATFB, 98%) was from Acros Organics. Ethanol (99.7%) was obtained from QRëC. Sodium dihydrogen phosphate (NaH$_2$PO$_4$) and disodium hydrogen phosphate (Na$_2$HPO$_4$) used in pH 7 phosphate buffer solution preparation were purchased from Bendosen Laboratory Chemicals. Deionized (DI) water with a resistivity of 18.2 MΩ cm from a Millipore Direct-Q3 purification water system was used in all preparation of electrochemical solutions.

[z]E-mail: hishamhamzah@usm.my

Electrografting of Boc-HDA onto GC electrodes.—Before the electrografting process, GC electrodes (3 mm OD, 0.071 cm^2) were polished until a mirror finish was obtained. The polishing and electrografting procedures followed the steps that have been reported previously.[3,12] The electrochemical attachment of Boc-HDA linker to the electrode surface was performed by electrochemical oxidation in 15 mM *N*-Boc-1,6-hexanediamine solution in acetonitrile containing 0.1 M TBATFB as the supporting electrolyte. The electrode potential was swept from 0.0 to 2.0 V *vs.* Ag/AgCl for 7 cycles at 50 mV s^{-1}. The Boc protecting group was then removed by immersing the modified electrodes in 4 M HCl in dioxane for 1 h. The modified electrodes were then rinsed thoroughly with deionized water and ethanol. They were then let to dry before conducting the electrochemical characterization.

Electrochemical characterization of HDA modified GC electrodes.—All electrochemical experiments were conducted in an electrochemical glass cell containing a 0.1 M KCl or 0.1 M phosphate buffer (pH 7) solution at room temperature placed inside a Faraday cage. The CV and EIS were recorded using an Autolab PGSTAT204 potentiostat/galvanostat (Ecochemie). An Ag/AgCl and a platinum gauze (1 × 0.5 cm^2) were utilized as the reference and counter electrode, respectively. All electrochemical experiments were carried out in the two aforementioned electrolytes without O$_2$ saturation since the aim of this work was to investigate the intrinsic behaviour of dissolved O$_2$ in stagnant aqueous electrolytes. The electrochemical data were treated and analyzed using Origin 9.1 software. The EIS fittings were performed using NOVA 1.11 software (Metrohm Autolab). Besides, all statistical differences between datasets were analyzed using an unpaired student *t*-test on GraphPad Prism 5.0. The data were presented as mean ± standard deviation (SD) and p < 0.05 was considered as significant.

Results and Discussion

Electrocatalytic behaviour of HDA modified GC electrodes.—When electrografting Boc-HDA onto the electrode surface, it has been reported that a broad irreversible oxidation peak on the first cycle of the recorded CV is observed at around 1.6 V *vs.* Ag/AgCl.[9,13] Nonetheless, the size of the oxidation peak decreases until it completely disappears as the potential was cycled continuously as shown in Fig. S1 (supplementary information is available online at stacks.iop.org/JES/167/166508/mmedia). This indicates that a monolayer film of Boc-HDA linker has entirely passivated the GC electrode surface. Then, ORR was studied using the obtained

Boc-HDA film in neutral electrolyte media. Figure 1A shows the CVs for the ORR recorded by employing Boc-HDA modified GC (orange), HDA modified GC (black), and bare GC (blue) electrodes in an unpurged 0.1 M KCl solution. Only the first CV cycle recorded at each electrode was used in our analysis as it corresponds to the exact amount of dissolved O$_2$ in the solution. For comparison, a voltammetric response was also acquired using a bare GC in a deoxygenated KCl solution (red) whilst blanketing the solution with a constant flow of N$_2$. Interestingly, the current for the ORR is significantly enhanced when utilizing the HDA modified GC electrode (i.e. in the absence of Boc group) as demonstrated by the black voltammogram; the potential for the cathodic peak has shifted to a more positive value at around −0.42 V compared to the bare GC and Boc-HDA modified electrodes.

It is interesting to note that catalytic reaction sites for ORR are formed by a HDA monolayer film. This could be due to O$_2$ molecules being adsorbed on their sides, orientated by nitrogen-induced charge delocalization from amino groups. Therefore, an HDA monolayer film could provide active sites for the ORR. We propose that the two amino groups on the attached HDA linker make an adjacent carbon atom highly positively charged, thus creating a Lewis basic site.[14] However, we strongly believe that the primary amino group located at the end of the attached linker can be an active site for the ORR, as shown in Scheme 1. This is demonstrated by the CV response of the Boc-HDA modified GC electrode (orange curve in Fig. 1A), which does not present any significant improvement of voltammogram shape compared to the bare GC electrode (blue curve). The primary amine (–NH$_2$) would activate an O$_2$ molecule chemisorbed to the C$^{\delta+}$ via end-on adsorption rather than side-on adsorption. This would significantly weaken the O-O bond, thus increasing the ORR activity.[15]

To further investigate the ORR on the HDA modified GC electrode, voltammograms obtained in aerated (black) and deoxygenated (red) KCl solutions were compared as shown in Fig. 1B. The CVs demonstrate that the HDA monolayer film shows an improved electrocatalytic behaviour towards the ORR. To confirm the claim that the ORR electrocatalytic activity is enhanced by the HDA monolayer film, control experiments were carried out. For the control, all modification steps were kept constant as mentioned in the Experimental section, however, without molecular Boc-HDA in the supporting electrolyte used for electrografting. Cyclic voltammograms for the ORR in 0.1 M KCl were recorded both after the first (cycling the electrode potential in acetonitrile containing only TBATFB) and the second (immersion in 4 M HCl in dioxane) modification steps. The CV responses from the control experiments
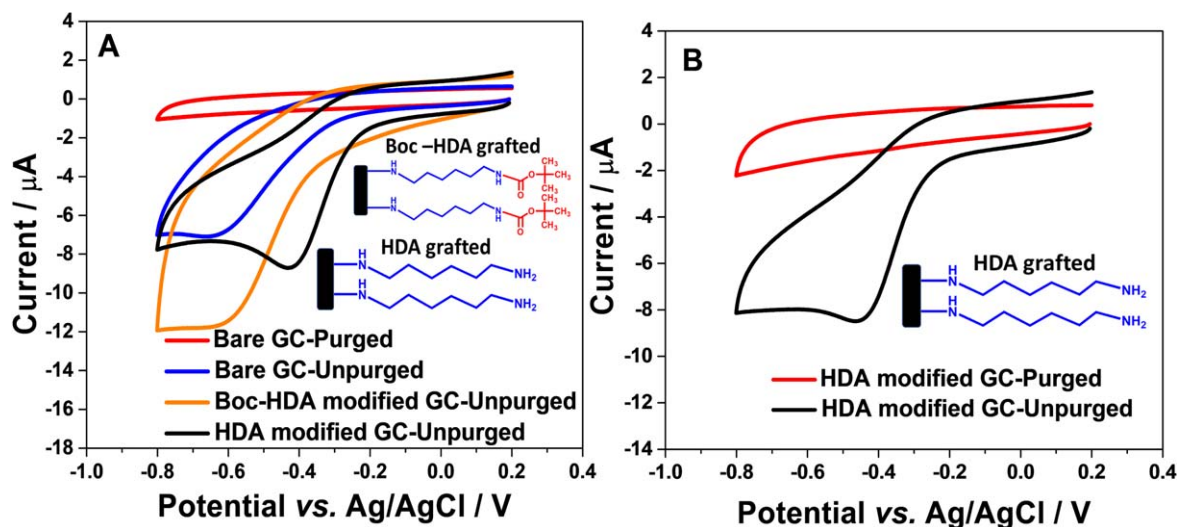

Figure 1. (A) Voltammetric responses for ORR (1st scan shown), recorded at 50 mV s^{-1} using bare, Boc-HDA modified, HDA modified GC electrodes in an unpurged 0.1 M KCl solution. CV in red was obtained from a bare GC electrode after degassing the KCl solution with N$_2$. (B) Comparison of CVs (1st scan shown) acquired at a HDA modified GC electrode in purged and unpurged 0.1 M KCl solutions, recorded at 50 mV s^{-1}.
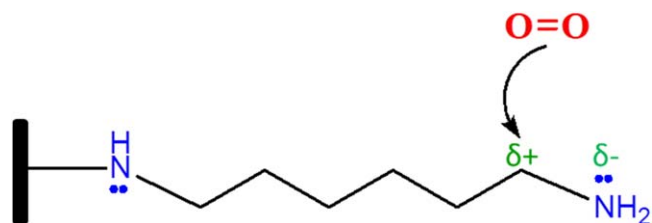
Scheme 1. Representation of the proposed catalytic site for the chemisorption of molecular O_2 for the ORR activity at the HDA monolayer film via π bond interactions.

were compared to the ones obtained at the Boc-HDA modified and HDA modified GC electrodes (Fig. 2A). Looking at the CV responses, the ORR current recorded at the bare GC electrode after modification step 1 (black CV) is bigger than that of the HDA modified GC electrode (red CV). This result is expected since cycling the electrode potential at positive values would alter the morphology of the electrode surface, roughening it and resulting in an increased number of electroactive sites. The roughened surface would also present a higher capacitive/background current. In contrast, the ORR response from the bare GC electrode after modification step 2 (green CV) shows a lower current intensity, probably due to the treatment in 4 M HCl in dioxane, which would make the electrode surface less roughened or blocked by dioxane. This can be explained by the significantly decrease of the capacitive current when compared to that of the bare GC electrode after modification step 1 (compare green and black CVs). It is interesting that cycling freshly polished GC electrodes in acetonitrile from 0 to 2 V *vs.* Ag/AgCl results in roughening the GC surface. However, to support this statement, further studies are needed, for example investigating the surface morphology of the electrodes by FE-SEM or AFM. Besides, XPS measurements could also be used to understand if the electrochemical treatment would form an oxide film at the GC surface.

Although the ORR current intensity of the bare GC electrode after modification step 1 is higher than that of the HDA modified GC electrode, due to the roughening of the electrode surface, however, the cathodic peak potential (E_{pc}) of the HDA modified GC electrode

is smaller than that of the treated bare GC electrode (see Fig. 2B). From the statistical analysis, a significant difference between the E_{pc} of the HDA modified GC electrode ($p < 0.001$) and that of the treated bare GC electrode (after modification step 1) was found. This indicates that the HDA film had provided better catalytic sites for the ORR activity than the roughened GC surface, by lowering the ORR overpotential. This may be due to i) lower activation energies[16] by the increased stability of molecular O_2 at the catalytic sites of the HDA layer during the chemisorption process, ii) lower binding energies of molecular O_2[16] towards the active sites at the HDA film, and iii) better mass transport[17] as the presence of the HDA layer makes easier the diffusion of molecular O_2 into and out of the catalytic sites. However, it is difficult to draw a solid conclusion from the present study as several thermodynamic and kinetic parameters would need further investigation, such as the standard potential, the diffusion coefficient, the surface coverage of adsorbed O_2, the rate constant for adsorption, the rate constant for the homogenous reaction, the electron transfer rate, and the transfer coefficient (α) for the ORR.

To investigate the stability of the HDA monolayer film towards the ORR, 10 cycles of CV were scanned as shown in Fig. 3. The CV shows that, after three cycles, the current stabilizes as the oxygen concentration profile has been set up at the electrode surface. This can be further explored by using Digital simulation programs such as DigiElch and Digisim. However, it is beyond the scope of the present study.

We have also probed the ORR in a phosphate buffer (PB) solution (pH 7) as demonstrated in Fig. 4A. It seems that the cathodic current acquired using the HDA modified GC electrode in PB solution (red) is of the same magnitude as the one recorded in a KCl solution (black). The currents for both datasets from three different HDA modified electrodes were compared as depicted in Fig. 4B.

Additionally, through statistical analysis using a student *t*-test, no significant differences were found when comparing the cathodic peak currents measured in the two solutions (KCl and PB). Furthermore, as platinum metal is widely-known as a good metal catalyst for the ORR,[18] the voltammetric response obtained using a bare Pt electrode (2 mm OD, 0.0341 cm^2) in an aerated KCl solution was compared to that acquired at a HDA film, as shown in Fig. 4C.
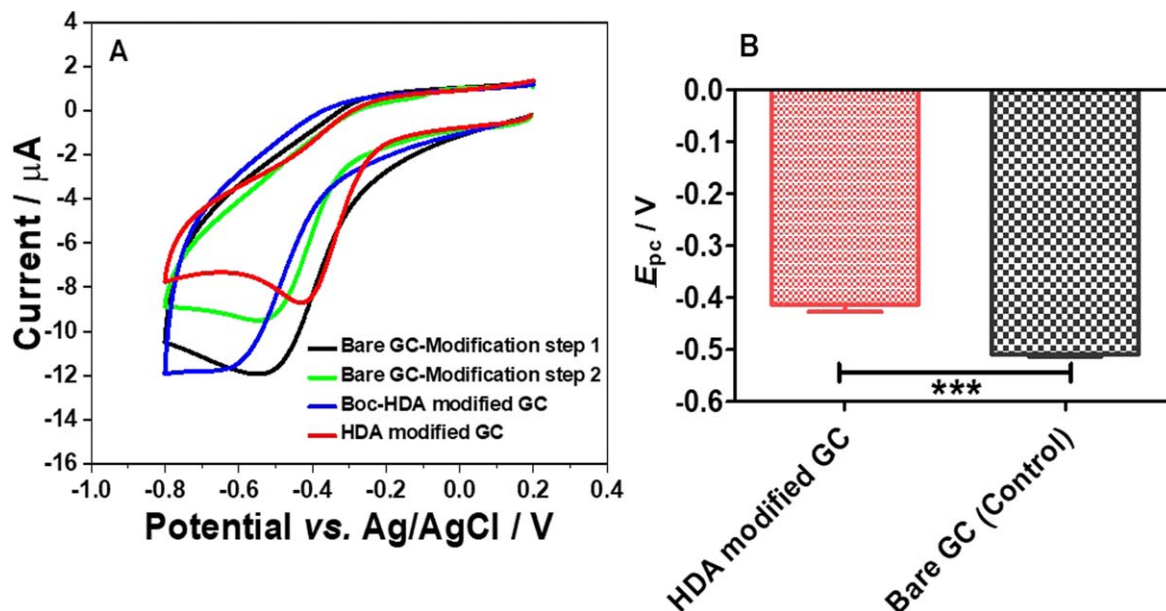

Figure 2. (A) Voltammetric responses for ORR (1st scan shown) recorded at a bare GC electrode (control) after modification step 1 (electrochemical treatment) and modification step 2 (acid treatment), a Boc-HDA modified GC electrode and a HDA modified GC electrode. The measurements were performed in unpurged 0.1 M KCl solution at a scan rate of 50 mV s^{-1}. (B) Bar graph reporting the cathodic peak potential (E_{pc}) for ORR obtained at bare GC (after modification step 1) and HDA modified GC electrodes. Statistical analysis was performed using an unpaired student *t*-test. Data are shown as mean ± S.D., n = 3 and *** denotes $p < 0.001$.
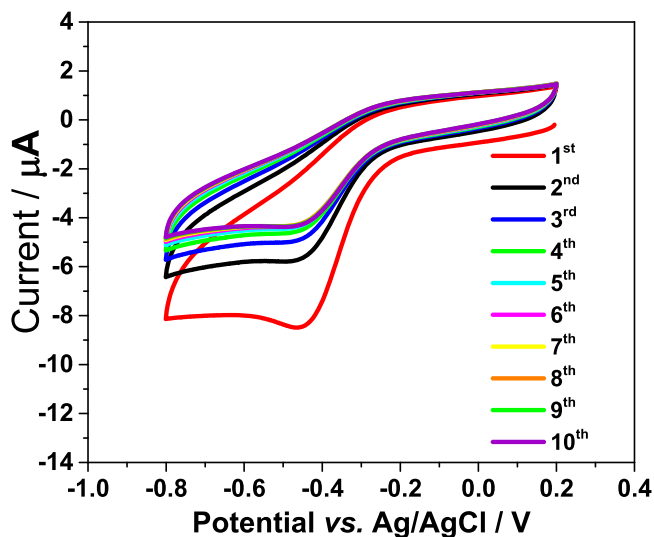
Figure 3. Ten cyclic voltammetry scans recorded at a HDA modified GC electrode for ORR in an unpurged 0.1 M KCl solution, recorded at 50 mV s^{-1}.

Although the onset potential for the ORR obtained at the bare Pt electrode is 0.21 V smaller (or at more positive potentials) than that of the HDA modified GC electrode (at $-0.10\,\text{mA cm}^{-2}$), the cathodic current density of the HDA film is undeniably higher than that of the bare Pt electrode, as illustrated in Figs. 4C and 4D. From the student *t*-test (Fig. 4D), a significant difference between the cathodic current densities of the HDA modified GC electrode ($p < 0.001$) and the bare Pt electrode was found. This implies that the HDA film offers excellent ORR electrocatalytic properties with only 0.21 V higher onset potential, compared to bare Pt electrodes, in aqueous neutral media.

Characterization of HDA modified GC electrodes by EIS.— Since the CVs for ORR in Fig. 1 were obtained in a stagnant solution, the physicochemical processes of the ORR at the electrode/electrolyte interface was investigated using EIS. This is because EIS is an effective technique to examine the electrochemical reactions occurring at the electrode interface in stagnant solutions by fitting the EIS spectra to appropriate electrochemical equivalent circuits.[19] For this work, EIS was measured at four different potentials chosen based on the CV data: +0.1, −0,1, −0.2, and −0.35 V *vs*. Ag/AgCl as shown in the Nyquist and Bode plots, Figs. 5A and 5B, respectively. As the onset potential for the HDA modified GC
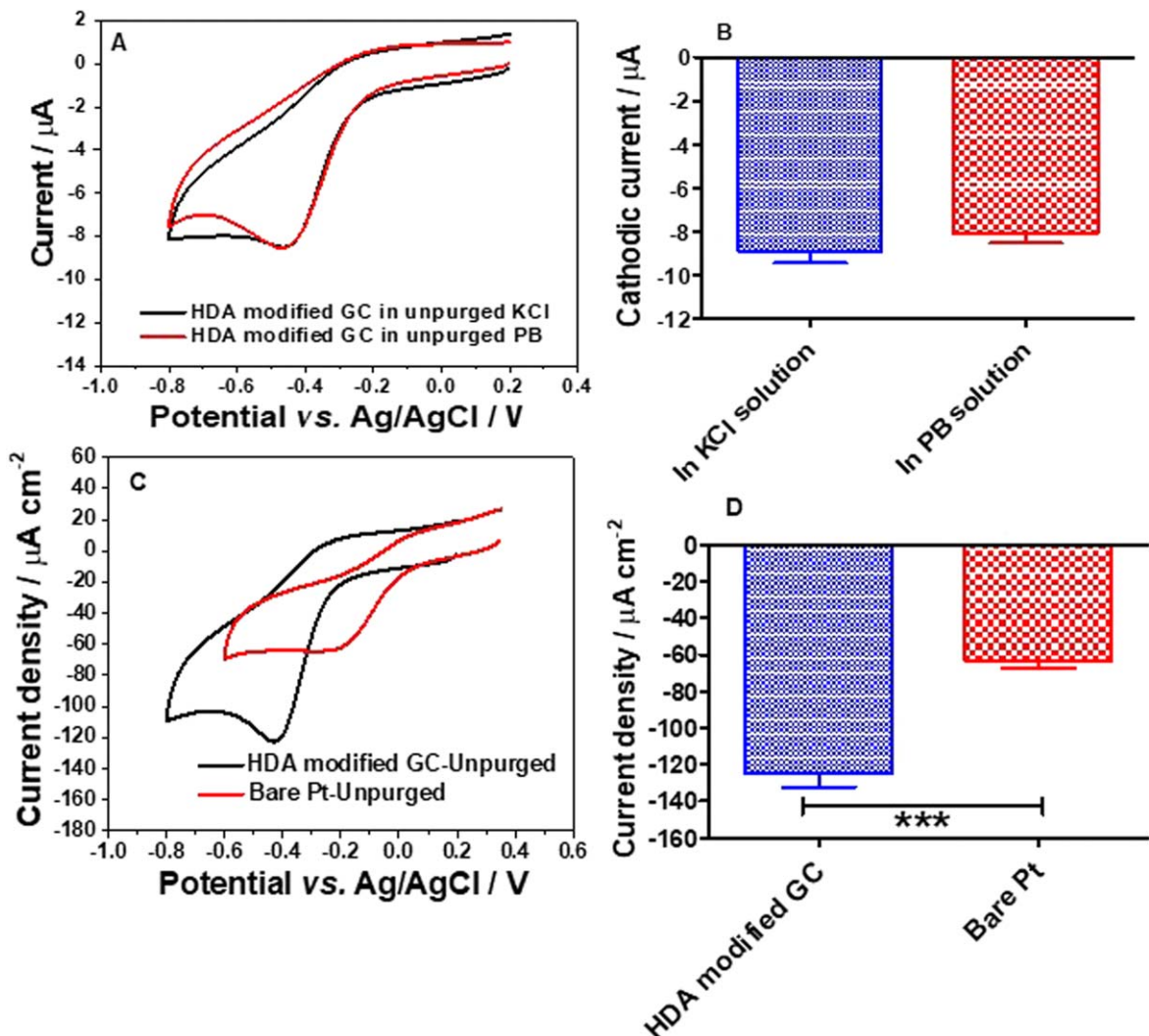

Figure 4. (A) Comparison of electrocatalytic currents from CVs (1st scan shown) recorded at HDA modified GC electrodes in unpurged 0.1 M KCl and 0.1 M PB (pH 7) solutions at a scan rate of 50 mV s^{-1}. (B) Bar graph comparing the cathodic peak current (i_{pc}) for ORR measured in unpurged 0.1 M KCl and 0.1 M PB (pH 7) solutions. (C) Comparison of electrocatalytic current densities from CVs (1st scan shown) recorded at a HDA modified GC electrode and a bare Pt electrode in unpurged 0.1 M KCl solution. (D) Bar graph comparing the cathodic current densities for HDA modified GC electrodes and bare Pt electrodes in unpurged 0.1 M KCl solution. Statistical analyses were performed using an unpaired student *t*-test. Data are shown as mean ± S.D., n = 3 and *** denotes $p < 0.001$.
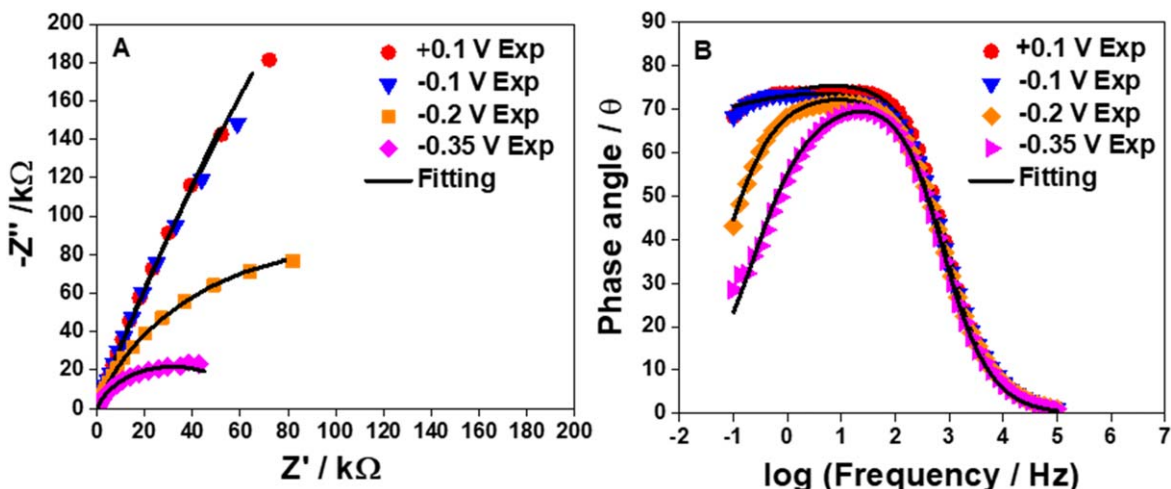
Figure 5. EIS measurements for HDA modified GC electrode in an unpurged 0.1 M KCl solution at different potentials, namely +0.1, −0.1, −0.2, and −0.35 V *vs*. Ag/AgCl. (A) Experimental and fitted data of Nyquist plots. (B) Experimental and fitted data of Bode plots. EIS was measured at an amplitude of 5 mV with frequencies between 100 kHz and 0.01 Hz.

electrode was estimated to be ∼−0.19 V *vs*. Ag/AgCl, two different potential sets for EIS were chosen to investigate the physicochemical processes of the ORR activity at the electrode interface, namely before (+0.1 and −0.1 V) and after (−0.2 and −0.35 V) the onset potential (∼−0.19 V). In fact, in the region before the onset potential, the dissolved O_2 in the electrolyte solution should diffuse from the bulk solution to the electrode surface. On the other hand, beyond the onset potential, O_2 molecules will be chemisorbed at the catalytic sites of the HDA monolayer to undergo the reduction reaction.

Two different equivalent circuits have been modelled as illustrated in Figs. 6A and 6B to convergently fit the experimental EIS spectra so as to understand the electrocatalytic behaviour of the ORR at the HDA monolayer film.

The electrochemical circuit in Fig. 6A fits well to the EIS spectra obtained at +0.1 and −0.1 V, where the goodness-of-fit (x^2) values are 0.00195 and 0.0155, respectively. Clearly, the physical process is mainly controlled by the diffusion process at both potentials as indicated by the presence of the Warburg impedance element (W) on the circuit model. This signifies that at +0.1 and −0.1 V, dissolved O_2 molecules diffuse from the bulk of the electrolyte to the active HDA catalytic sites. In contrast, the circuit shown in Fig. 6B is the best fitted to the semicircle-shaped EIS spectra at −0.2 and −0.35 V, giving the x^2 values of 0.008 and 0.030, respectively. The equivalent circuits suggest that the interfacial processes at both potentials are principally controlled by the kinetic transfer process, also known as charge transfer resistance (R_{ct}). This means that dissolved O_2 molecules are adsorbed at the electrode surface at −0.2 and −0.35 V to undergo a further reduction process. Besides, the size of the semicircles for the EIS spectra (Fig. 5A) decreases as the applied potential is set to more negative values from −0.2 to −0.35 V. It can be concluded that the R_{ct} at −0.35 V is lower than that at −0.2 V. This result is in line with the R_{ct} values obtained from the equivalent circuits for both potentials (see Tables SIII and SIV). Moreover, based on the data trend obtained from the Bode plots (Fig. 5B), the values of phase angle at low frequency decreases as the applied potential becomes more negative from +0.1 to −0.35 V. The Bode plots at low frequency can be associated to the adsorbed O_2 molecules or to the accumulation of intermediate species from the ORR. The decreasing trend of the Bode plots at low frequency indicates the changes in the values of R_{ct} and C_{dl} for the interfacial processes. This can be seen by the shift of the maximum values of the phase angle in the Bode plots as the spectra are scanned from a low-frequency region to a medium-frequency region when measuring the EIS spectra from +0.1 to −0.35 V. All the values of the fitting parameters at different potentials are presented in Tables
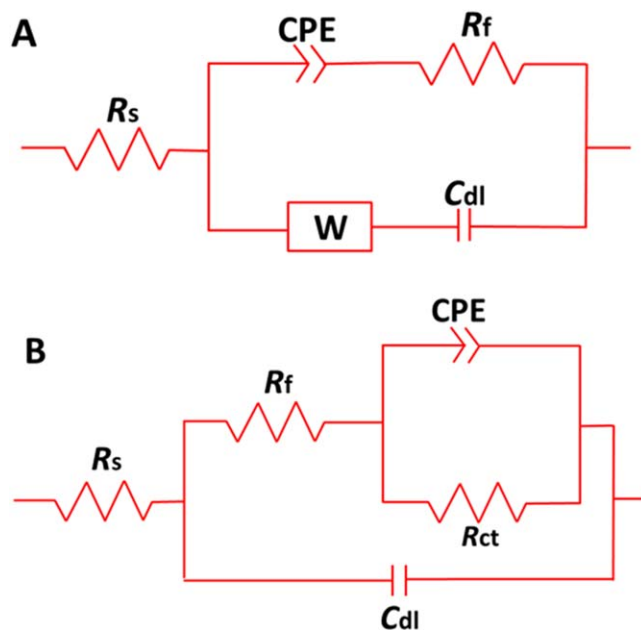

Figure 6. Suggested equivalent electrochemical circuits utilized to fit Nyquist and Bode plots at (A) +0.1 and −0.1 V *vs*. Ag/AgCl, and (B) −0.2 and −0.35 V *vs*. Ag/AgCl. R_s is the solution resistance, W is the Warburg impedance element, C_{dl} is the double-layer capacitance, CPE is the constant phase element, representing the HDA film capacitance, R_f is the HDA film resistance, and R_{ct} is the charge transfer resistance controlled by the electron transfer kinetics.

SI–SIV. From the equivalent circuits, it can be concluded that the physicochemical processes for the ORR at the HDA film are controlled by both diffusion and adsorption processes. To support this conclusion, CV measurements at different scan rates were carried out which will be discussed in the next section.

CV scan rate studies.—Cyclic voltammetry studies were performed by varying the scan rate between 60 and 250 mV s^{-1} as shown in Fig. 7A. The scan rate studies can reveal whether the electrocatalytic activity towards the ORR shown by the HDA monolayer is controlled by diffusion, adsorption, or even both processes. The cathodic peak current (i_{pc}) was plotted against the square root of scan rate (v)$^{1/2}$ (Fig. 7B) and against the scan rate (v) (Fig. 7C).
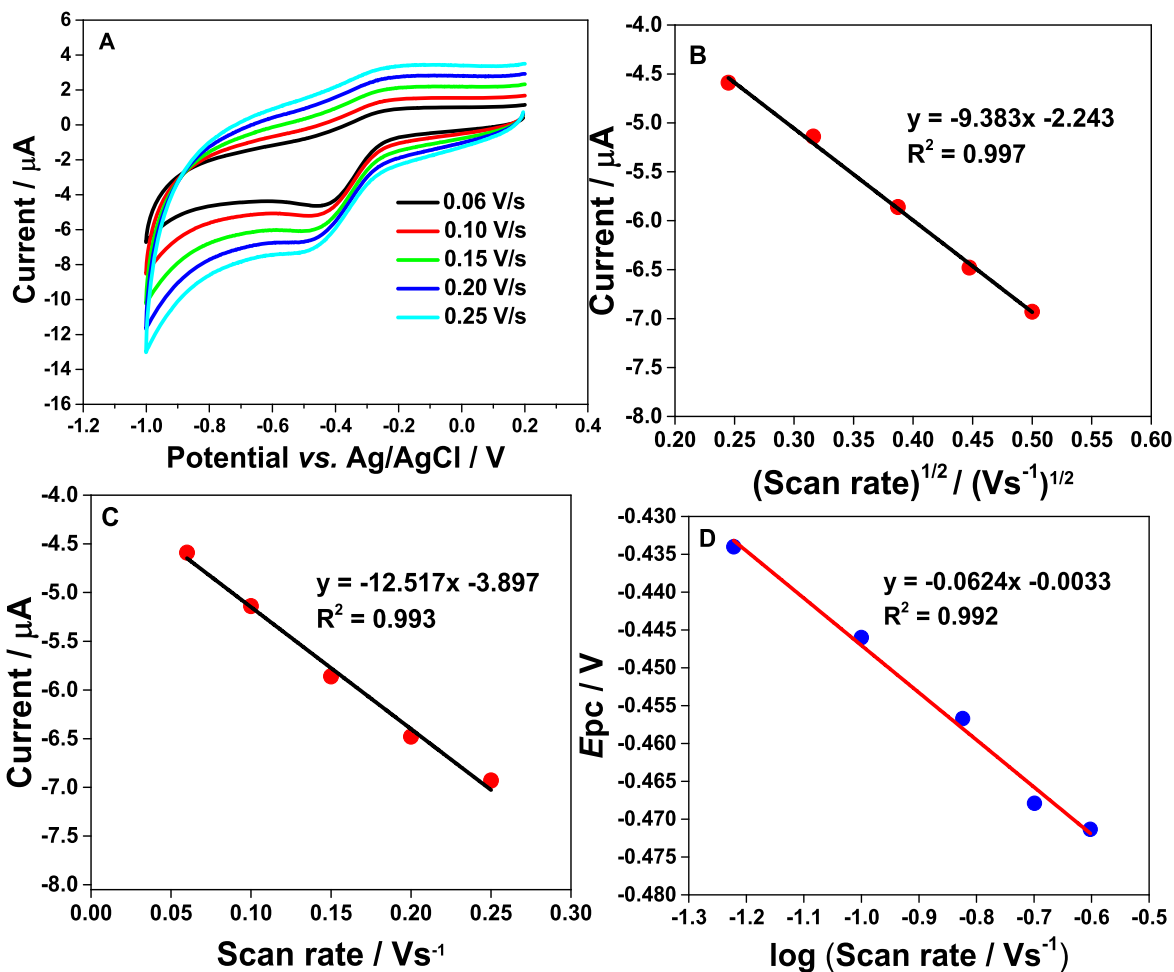
Figure 7. (A) CVs at different scan rates for ORR at a HDA modified GC electrode in an unpurged 0.1 KCl solution (scan rate goes from 0.06 to 0.25 V s^{-1}). (B) Linear dependence of the cathodic peak current *vs.* the square root of the scan rate ($v^{1/2}$). (C) Linear dependence of the cathodic peak current *vs.* scan rate (v). (D) Plot of the cathodic peak potential (E_{pc}) *vs.* log(scan rate).

Figures 7B and 7C show linear relationships between the cathodic peak current and both the $v^{1/2}$ as well as v. A linear response for the peak current *vs.* $v^{1/2}$ is a typical trend for diffusion-controlled reactions. Nonetheless, the peak current also presents a linear correlation with v which implies the presence of adsorbed electroactive species. These findings suggest that the ORR at the HDA modified GC electrode is a mixture of diffusion- and kinetic-controlled reactions that involve the adsorption of O_2 molecules at the electrode surface. This conclusion is in agreement with the results obtained from the EIS measurements. Additionally, the number of electrons (n) involved in the electrocatalytic reaction can be calculated using the following Laviron equation for irreversible CV behaviour,[20]

$$E_{pc} = E^{0'} \left(\frac{2.303RT}{\alpha nF} \right) \log \left(\frac{RTk^{\circ}}{\alpha nF} \right) + \left(\frac{2.303RT}{\alpha nF} \right) \log v \qquad [1]$$

where E_{pc} is the cathodic peak potential, $E^{0'}$ is the formal redox potential, R is the gas constant, T is the temperature in Kelvin, α is the transfer coefficient, F is the Faraday constant, and k° is the standard heterogeneous rate constant of the reaction. Based on Eq. 1, E_{pc} was plotted *vs.* log(v) as depicted in Fig. 7D where a linear relationship is observed. From the slope of the linear fit, the value of αn can be calculated, which was found to be 0.927 ± 0.037. Nissim and Compton[21] reported that the value of α for the ORR in an oxygenated 0.1 M KCl solution using a GC electrode was 0.24. Therefore, the value of n for the ORR at HDA films was calculated to be 3.87 ± 0.19 (as average of 3 modified electrodes) when using α

= 0.24. This value of n is very close to 4 which means that the dissolved oxygen molecules are directly reduced to water without forming hydrogen peroxide as an intermediate product.[22] Moreover, the k° value can also be calculated from Eq. 1. To do that, the value of $E^{0'}$ was first obtained by extrapolation from a plot of E_{pc} against v. The k° value for the ORR was found to be 1.91 ± 0.39 s^{-1}. This also suggests that the ORR at the HDA monolayer film proceeds with a fast kinetic transfer step, implying that the dissolved O_2 molecules are completely reduced to water without generating hydrogen peroxide (H_2O_2) as an intermediate species. Thus, it can be concluded that the HDA film can be an excellent candidate as heterogeneous catalyst for the ORR. As the number of the electrons transferred was calculated as 4, we can assume that the ORR mechanism at the HDA monolayer is the one illustrated in Scheme 2. Such a mechanism has already been proposed by Nakamura et al.[23]

Since the values of diffusion coefficient *(D)* and α can be obtained from literature, the concentration (C) of dissolved O_2 could be determined from the slope of the graph of current *vs.* $v^{1/2}$ (Fig. 7B) by using the Randles-Sevcik equation.[24] The slope is given by:

$$|Slope| = (2.99 \times 10^5) \, n^{\frac{3}{2}} \, \alpha^{\frac{1}{2}} A C D^{\frac{1}{2}} \qquad [2]$$

where A is the electrode area. By using the D value of 1.92×10^{-6} cm^2 s^{-1}, reported by Zing et al.,[25] the C of dissolved O_2 was calculated to be $1.07 \pm 0.071 \times 10^{-7}$ mol cm^{-3}. The magnitude of the O_2 concentration obtained in this work is close to the typical concentration of dissolved oxygen in aerated solutions, which is
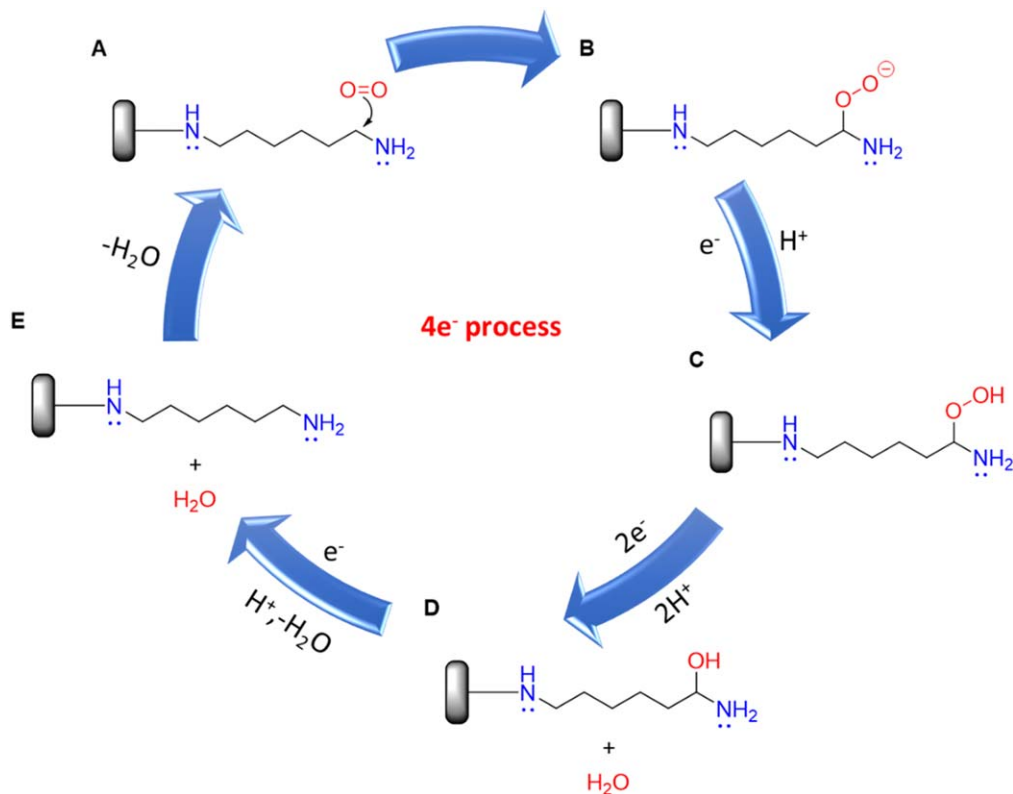
Scheme 2. The proposed ORR mechanism pathway at the HDA monolayer electrografted on the GC electrode surface.

2.5×10^{-7} mol cm^{-3}.[26] This shows the high potential of this modified electrode for the ORR.

Conclusions

This work shows that HDA films electrografted at GC electrodes enhanced the electrocatalytic activity towards the ORR, which has never been reported by other studies. From the CV responses, it was found that the HDA modified GC electrode exhibited a higher reduction current density than a bare Pt electrode, although its onset potential lags the bare Pt by 0.21 V. Through EIS measurements at different potentials, the ORR was determined to be governed by both mass and charge transfer steps. The results from EIS were confirmed by those obtained by the scan rate studies. Additionally, the ORR was found to proceed via a four-electron pathway mechanism and fast kinetic transfer step based on the Laviron analyses. This is a remarkably interesting finding because a grafted HDA film can also be an alternative heterogeneous catalyst for the ORR, opening a new route to further understand the fundamental mechanisms of the ORR. This type of electrode is preferable as it can eliminate the use of enzymes which can be expensive, unstable, and inefficient. The results obtained from this study show a big potential for the development of dissolved O$_2$ sensors or fuel cells.

ORCID

Hairul Hisham Hamzah https://orcid.org/0000-0002-8296-1360
Marta Meneghello https://orcid.org/0000-0003-0099-1783
Saiful Arifin Shafiee https://orcid.org/0000-0003-0907-624X
Turgut Sönmez https://orcid.org/0000-0002-3927-2551
Mohamad Nurul Azmi Mohamad Taib https://orcid.org/0000-0002-2447-0897

References

1. D. Bélanger and J. Pinson, "Electrografting: a powerful method for surface modification." *Chem. Soc. Rev.*, **40**, 3995 (2011).
2. P. Allongue, M. Delamar, B. Desbat, O. Fagebaume, R. Hitmi, J. Pinson, and J.-M. Savéant, "Covalent modification of carbon surfaces by aryl radicals generated from the electrochemical reduction of diazonium salts." *J. Am. Chem. Soc.*, **119**, 201 (1997).
3. H. H. Hamzah, W. C. Chein, S. S. F. Rahiman, and S. A. Shafiee, "Investigating the effects of primary amine linkers with different carbon chain lengths on the acid dissociation constant (p*K*a) for covalently immobilized anthraquinone at the electrode surface using linear and non-linear fittings." *J. Electrochem. Soc.*, **166**, H877 (2019).
4. M. Sosna, J.-M. Chrétien, J. D. Kilburn, and P. N. Bartlett, "Monolayer anthracene and anthraquinone modified electrodes as platforms for trametes hirsuta laccase immobilisation." *Phys. Chem. Chem. Phys.*, **12**, 10018 (2010).
5. F. A. Al-Lolage, M. Meneghello, S. Ma, R. Ludwig, and P. N. Bartlett, "A flexible method for the stable, covalent immobilization of enzymes at electrode surfaces." *Chem. Electro. Chem.*, **4**, 1528 (2017).
6. A. Adenier, M. M. Chehimi, I. Gallardo, J. Pinson, and N. Vilà, "Electrochemical oxidation of aliphatic amines and their attachment to carbon and metal surfaces." *Langmuir*, **20**, 8243 (2004).
7. H. H. Hamzah, G. Denuault, P. N. Bartlett, A. Pinczewska, and J. D. Kilburn, "Electrografting of mono-N-Boc-ethylenediamine from an acetonitrile/aqueous NaHCO3 mixture." *J. Electrochem.*, **23**, 130 (2017).
8. H. Randriamahazaka and J. Ghilane, "Electrografting and controlled surface functionalization of carbon based surfaces for electroanalysis." *Electroanalysis.*, **28**, 13 (2016).
9. M. A. Ghanem, J.-M. Chrétien, A. Pinczewska, J. D. Kilburn, and P. N. Bartlett, "Covalent modification of glassy carbon surface with organic redox probes through diamine linkers using electrochemical and solid-phase synthesis methodologies." *J. Mater. Chem.*, **18**, 4917 (2008).
10. M. Meneghello, F. A. Al-Lolage, S. Ma, R. Ludwig, and P. N. Bartlett, "Studying direct electron transfer by site-directed immobilization of cellobiose dehydrogenase." *ChemElectroChem.*, **6**, 700 (2019).
11. F. A. Al-Lolage, P. N. Bartlett, S. Gounel, P. Staigre, and N. Mano, "Site-directed immobilization of bilirubin oxidase for electrocatalytic oxygen reduction." *ACS Catal.*, **9**, 2068 (2019).
12. J. Groppi, P. N. Bartlett, and J. D. Kilburn, "Toward the control of the creation of mixed monolayers on glassy carbon surfaces by amine oxidation." *Chem. - A Eur. J.*, **22**, 1030 (2016).
13. J.-M. Chrétien, M. A. Ghanem, P. N. Bartlett, and J. D. Kilburn, "Covalent tethering of organic functionality to the surface of glassy carbon electrodes by using electrochemical and solid-phase synthesis methodologies." *Chem. - A Eur. J.*, **14**, 2548 (2008).

14. Y. Li, Q. Li, H. Wang, L. Zhang, D. P. Wilkinson, and J. Zhang, "Recent progresses in oxygen reduction reaction electrocatalysts for electrochemical energy applications." *Electrochem. Energy Rev.*, **2**, 518 (2019).

15. K. Gong, F. Du, Z. Xia, M. Durstock, and L. Dai, "Nitrogen-doped carbon nanotube arrays with high electrocatalytic activity for oxygen reduction." *Science*, **323**, 760 (2009).

16. A. Kulkarni, S. Siahrostami, A. Patel, and J. K. Nørskov, "Understanding catalytic activity trends in the oxygen reduction reaction." *Chem. Rev.*, **118**, 2302 (2018).

17. Z. J. Jiang and Z. Jiang, "Reduction of the oxygen reduction reaction overpotential of nitrogen-doped graphene by designing it to a microspherical hollow shape." *J. Mater. Chem. A.*, **2**, 14071 (2014).

18. S. Sui, X. Wang, X. Zhou, Y. Su, S. Riffat, and C. Liu, "A comprehensive review of Pt electrocatalysts for the oxygen reduction reaction: nanostructure, activity, mechanism and carbon support in PEM fuel cells." *J. Mater. Chem. A.*, **5**, 1808 (2017).

19. M. Negem, H. Nady, and M. M. El-Rabiei, "Nanocrystalline nickel–cobalt electrocatalysts to generate hydrogen using alkaline solutions as storage fuel for the renewable energy." *Int. J. Hydrogen Energy*, **44**, 11411 (2019).

20. E. Laviron, "General expression of the linear potential sweep voltammogram in the case of diffusionless electrochemical systems." *J. Electroanal. Chem. Interfacial Electrochem.*, **101**, 19 (1979).

21. R. Nissim and R. G. Compton, "Nonenzymatic electrochemical superoxide sensor." *ChemElectroChem.*, **1**, 763 (2014).

22. T. Sönmez, S. J. Thompson, S. W. T. Price, D. Pletcher, and A. E. Russell, "Voltammetric studies of the mechanism of the oxygen reduction in alkaline media at the spinels Co_3O_4 and $NiCo_2O_4$." *J. Electrochem. Soc.*, **163**, H884 (2016).

23. D. Guo, R. Shibuya, C. Akiba, S. Saji, T. Kondo, and J. Nakamura, "Active sites of nitrogen-doped carbon materials for oxygen reduction reaction clarified using model catalysts." *Science*, **351**, 361 (2016).

24. Z. Zeng, W. Zhang, Y. Liu, P. Lu, and J. Wei, "Uniformly electrodeposited α-MnO_2 film on super-aligned electrospun carbon nanofibers for a bifunctional catalyst design in oxygen reduction reaction." *Electrochim. Acta*, **256**, 232 (2017).

25. H. T. Tsai, C.-Y. Yang, and S.-M. Chen, "Development of a dissolved oxygen sensor for commercial applications." *Int. J. Electrochem. Sci.*, **8**, 5250 (2013).

26. M. Bucko, P. Gemeiner, A. Vikartovská, D. Mislovicová, I. Lacík, and J. Tkáč, "Coencapsulation of oxygen carriers and glucose oxidase in polyelectrolyte complex capsules for the enhancement of D-gluconic acid and delta-glucono-lactone production." *Artif. Cells Blood Substit. Immobil. Biotechnol.*, **38**, 90 (2010).